Condensed Matter Physics, 2025, Vol. 28, No. 1, 13602: 1–16
DOI: 10.5488/CMP.28.13602
http://www.icmp.lviv.ua/journal

CONDENSED MATTER PHYSICS

On the temperature, pressure and composition effects in the properties of water-methanol mixtures. I. Density, excess mixing volume and enthalpy, and self-diffusion coefficients from molecular dynamics simulations

M. Cruz Sanchez [1], V. Trejos Montoya [1], O. Pizio [2*]

[1] Departamento de Química, Universidad Autónoma Metropolitana-Iztapalapa, Av. San Rafael Atlixco 186, Col. Vicentina, 09340, CDMX, México

[2] Instituto de de Química, Universidad Nacional Autónoma de México, Circuito Exterior, 04510, Cd. Mx., México

Received January 17, 2025, in final form February 10, 2025

We report the temperature, pressure and composition dependence of some basic properties of model liquid water-methanol mixtures. For this purpose the isobaric-isothermal molecular dynamics computer simulations are employed. Our principal focus is on the united atom non-polarizable UAM-I-EW model for methanol which was recently parametrized the paper by Garcia-Melgarejo et al. [J. Mol. Liq., 2021, **323**, 114576], combined with the TIP4P/ε water model. In perspective, the methanol model permits a convenient extension for other monohydric alcohols mixed with water. The behavior of density, excess mixing volume and enthalpy are described. Partial mixing properties are interpreted. Besides, we explored the trends of behavior of self-diffusion coefficients of the species of a mixture. The quality of predictions of the model is critically evaluated by detailed comparisons with experimental results. Various results are novel and provide new insights into the behavior of the mixtures in question at different temperatures and at high pressures. An improvement of the modelling necessary for further research is discussed.

Key words: *molecular dynamics simulation, water-methanol mixtures, partial molar volumes, excess enthalpy, self-diffusion coefiicients*

1. Introduction

The present work is an extension of our recent investigations of the properties of water-methanol liquid mixtures by using molecular dynamics computer simulations [1–4]. In contrast to those studies focused on the description of composition effects at room temperature and at ambient pressure, here we would like to explore the trends of behavior of various properties of water-methanol mixtures on temperature and pressure, besides the composition changes.

There is no need to say that water is essential for life and any kind of human activity. It remains to be a challenging research subject from the experimental and theoretical point of view. It exhibits several thermodynamic anomalies that still lack a definite profound explanation. The properties of water in both bulk phase and in mixtures are determined to much extent by changes of the hydrogen bonds network. Coexistence of water with organic matter determines our being. One of the principal phenomena within this "interface" is the hydrophobic effect. It refers to the extent of correlations between nonpolar or amphiphilic molecules (solutes) in aqueous media [5]. The strength of this effect depends on the intramolecular structure of solutes, solute-solvent (water) and solvent-solvent (water-water) interactions.

*Corresponding author: oapizio@gmail.com.

On the other hand, it depends on the chemical composition of the system as well as on temperature and pressure. This kind of phenomena has implications in physical chemistry and biology [6–8], as well as it is of crucial importance for academic research and for practical applications.

One of the simplest amphiphilic molecule types are alcohols, methanol between them in particular. Mixtures of alcohols with water have been studied in very many aspects by experimental and theoretical methods for a long time. This research has generated an enormous amount of literature, practically impossible to cite comprehensively. Most frequently, these systems were studied upon the changes of composition at room temperature and at ambient pressure. In spite of undoubtful importance, much less is known about the behavior of water-alcohol mixtures upon the changes of temperature and pressure, probably due to experimental difficulties. These issues are discussed in various publications [9–15].

Computer simulation techniques offer alternatives for laboratory research under such conditions [16–20]. They represent useful and popular tools to get profound insights into the microscopic structure, thermodynamic, dynamic, dielectric and interfacial properties of this type of systems. The most important, initial step of computer simulations methodology is in the design of an appropriate force field. The intramolecular structure of alcohol species is frequently considered at a united atom or all-atom level modelling of non-polarizable molecules. Unfortunately desirable, more sophisticated, polarizable force fields require much more expensive calculations. They are not comprehensively tested and much less frequently used at present. The appropriateness of the computer simulation predictions for a given model for a mixture, upon changing temperature, T, pressure, P, and composition, X, i.e., variables, should be tested by comparison with experimental data as much as possible. Several experimental techniques contributed to the understanding of the behavior of water-alcohol systems upon changes of temperature, pressure and composition. Namely, the neutron and dynamic light scattering, nuclear magnetic resonance, dielectric relaxation, vibrational, and Raman spectroscopy, calorimetry — all of them offer results that require support from computer simulations.

Profound insights into the properties of pure components of interest for the present study from computer simulations are available. Specifically, a comprehensive set of data for non-polarizable water models was provided by Vega and Abascal [21]. It is commonly accepted that the TIP4P/2005 is almost entirely successful model in a rather wide interval of thermodynamic parameters. A similar type of strategy of description was applied to methanol [22]. A substantial improvement of the dielectric constant for water was reached, however, by the development of the TIP4P/ε model [23]. Concerning a set of monohydric alcohols, the TraPPE data basis [24] has been frequently used to deal with individual species and aqueous solutions. Quite recently, this kind of united atom type modelling was critically reconsidered and revised to improve the solubility of alcohols in water [25]. As a result, the so-called UAM-I parametrization of alcohols model was combined with TIP4P/ε and tested at ambient pressure and temperature [25]. This kind of development was the subject of very recent study from this laboratory [26] to yield a rather comprehensive and successful description of mixtures of monohydric alcohols with water upon composition. Obviously, several combinations of water and alcohol models are necessary to explore more in detail. However, from a general perspective of various alcohols modelling, it seems interesting to investigate water-methanol mixtures upon temperature and pressure changes, besides composition. It may provide the first step of an ampler project involving a set of properties of various systems of this kind. Afterwards, one can undertake exploration of these mixtures using all-atom modelling for the sake of comparisons with united atom level and critical evaluation with experimental trends.

2. Models and simulation details

In this work we are principally interested in the united atom type, non-polarizable model with three sites, O, H, CH_3, parametrized very recently [25]. For water, the TIP4P/ε [23] model is considered. Nevertheless, in some parts of the manuscript we involve the united atom TraPPE methanol model [24] and the TIP4P/2005 water model. In general terms, within this type of modelling, the interaction potential between all atoms and/or groups is assumed as a sum of Lennard-Jones (LJ) and Coulomb contributions. Lorentz-Berthelot combination rules are used to determine the cross parameters for the relevant potential well depths and diameters.

Molecular dynamics computer simulations of water-methanol mixtures have been performed in the

isothermal-isobaric (NPT) ensemble at a given pressure and temperature values. We used GROMACS software [27] version 5.1.2. The simulation box in each run was cubic, the total number of molecules of both species in all cases is fixed at 3000. The composition of the mixture is described by the molar fraction of methanol molecules, $X_2 = N_2/(N_1 + N_2)$, where 1 and 2 refer to water and methanol species throughout this manuscript. As common, periodic boundary conditions were used. Temperature and pressure control has been provided by the V-rescale thermostat and Parrinello-Rahman barostat with $\tau_T = 0.5$ ps and $\tau_P = 2.0$ ps, the timestep was 0.002 ps. The value of $4.5 \cdot 10^{-5}$ bar^{-1} was used for the compressibility of mixtures.

The non-bonded interactions were cut-off at 1.4 nm, whereas the long-range electrostatic interactions were handled by the particle mesh Ewald method implemented in the GROMACS software package (fourth order, Fourier spacing equal to 0.12) with the precision 10^{-5}. The van der Waals correction terms to the energy and pressure were used. In order to maintain the geometry of water molecules and methanol intra-molecular bonds rigid, the LINCS algorithm was used.

After preprocessing and equilibration, consecutive simulation runs, each for not less than 10 ns, with the starting configuration being the last configuration from the previous run, were performed to obtain trajectories for the data analysis. The results for the majority of properties were obtained by averaging over 7–10 production runs. However, the self-diffusion coefficients were evaluated from the entire trajectory taking the best slope of the mean squared displacement as common.

3. Results and discussion

The first principal issue we would like to deal with is to evaluate the accuracy of predictions of the model for water-methanol mixture dependent on temperature, pressure and composition. This should be done for a set of target properties. The density is one of them. Therefore, we would like to begin this section by revisiting the dependence of density of individual species, water and methanol, on T, P and X_2, and then proceed to the mixture.

3.1. Density of water and methanol depending on temperature and pressure

The dependence of water density, ρ_1 on T has been the subject of very many reports using experimental methods and computer simulation approaches, in part because it exhibits an anomalous behavior. These studies were comprehensively described in [28]. Here, we involve recent measurements at high pressures and the relevant discussion from [29]. One of the first simulation studies that reported $\rho_1(T)$ curves at different pressures for TIP4P/2005 water model is from the laboratory of C. Vega, [30]. These authors explored an ample interval of temperatures, starting from $T \approx 375$ K down to deeply supercooled water. Four pressure values, $P = 1$ bar, 400 bar, 1000 bar and 1500 bar were considered. However, the simulations were performed for a small system of 256 and 500 molecules with cutoff of interactions at 0.9 nm, to obtain density and isothermal compressibility. Therefore, some of these simulations were redone for a bigger system using TIP4P/2005 model and a larger cutoff for inter-particle interaction, as noted above. However, the TIP4P/ε model is of our principal interest. Previous comparison of the predictions from TIP4P/2005 and TIP4P/ε was performed in [23] using 500 TIP4P/ε water molecules with $r_{\text{cut}} = 0.95$ nm. Actually, we would like to confirm some of the conclusions from [23].

Our calculations confirm three issues. Both water models, TIP4P/2005 and TIP4P/ε reproduce the experimental curve perfectly well. They underestimate water density at temperatures above 298.15 K very slightly (1a). The temperature of maximum density (TMD) is reproduced at $T = 276.15$ K for TIP4P/2005 model, the TIP4P/ε predicts it at almost the same temperature, 275.15 K. Moreover, both models correctly predict the shift of TMD to a lower temperature upon increasing pressure from 1 bar to 400 bar (1b). Apparently, the TIP4P/2005 is a bit superior to TIP4P/ε in this interval of parameters. On the other hand, if one considers the pressure dependence of density at $T = 298.15$ K and $T = 343.15$ K, then the TIP4P/ε model exhibits a better performance at rather high values of pressure (22).

Next, we performed simulations of pure methanol using the UAM-I and TraPPE united atom models. Both models describe the temperature dependence of density quite well at normal pressure, 1 bar, and at much higher pressure, 1000 bar (figure 3a). Nevertheless, the deviation of simulation results from

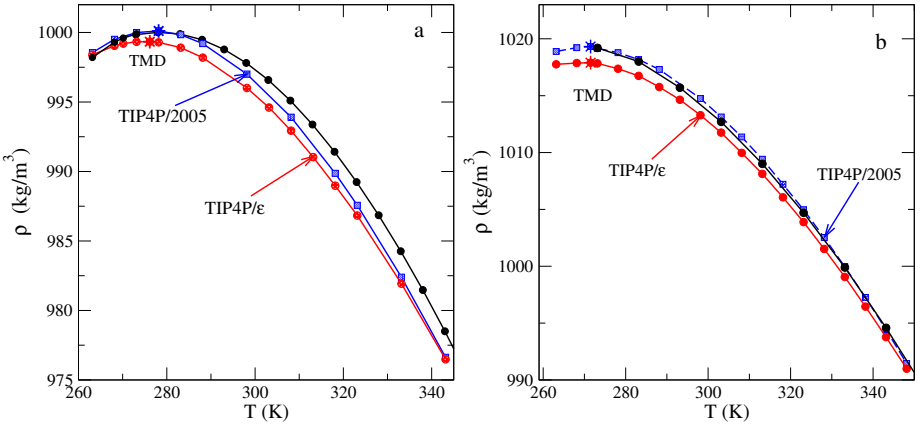

Figure 1. (Colour online) Water density depending on temperature at pressure 1 bar (panel a) and at 400 bar (panel b). Black circles denote experimental data. In panel a they are taken from [29], three experimental points at the lowest temperatures are from [31] for supercooled water. In panel b they come from [32]. The blue squares and red circles are our simulation results for TIP4P/2005 and TIP4P/ε models, respectively. Stars denote the temperature of maximum density (TMD).

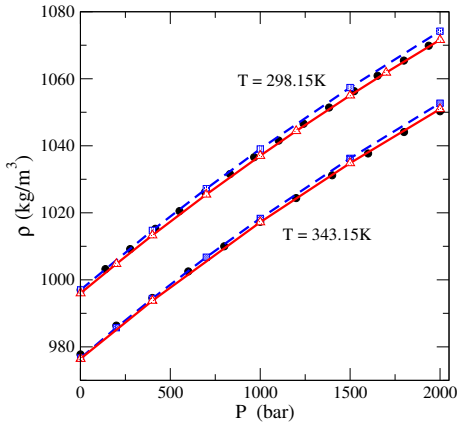

Figure 2. (Colour online) The dependence of water density on pressure at 298.15 K and at 343.15 K. The experimental data (black circles) are from [14] (298.15K) and NIST Chemistry Webbook (343.15 K) [33], respectively. The nomenclature of lines and symbols as in figure 1 (blue — TIP4P/2005, red — TIP4P/ε).

experimental data grows smoothly upon increasing temperature. At $P = 1$ bar, the TraPPE model is a bit better than the UAM-I. At a high pressure, however, the results of two models flow together. In panel b of this figure, figure 3b, the methanol density as a function of pressure is shown. Both methanol models reproduce $\rho(P)$ dependence very well. Deviation from the experimental data is rather small and decreases upon increasing pressure. In summary, we have confidence that two constituents of the mixtures in question, in their pure state, are well described.

3.2. Composition dependence of density of methanol-water mixtures at different temperatures and pressures

As we have mentioned in the introductory section, there have been several experimental reports concerning the density of water-methanol mixtures upon changing composition. We used experimental data at room temperature $T = 298.15$ K, and at atmospheric pressure [34]. At higher pressures, the experimental data are scarce. We have found solely the report by Kubota et al.[14].

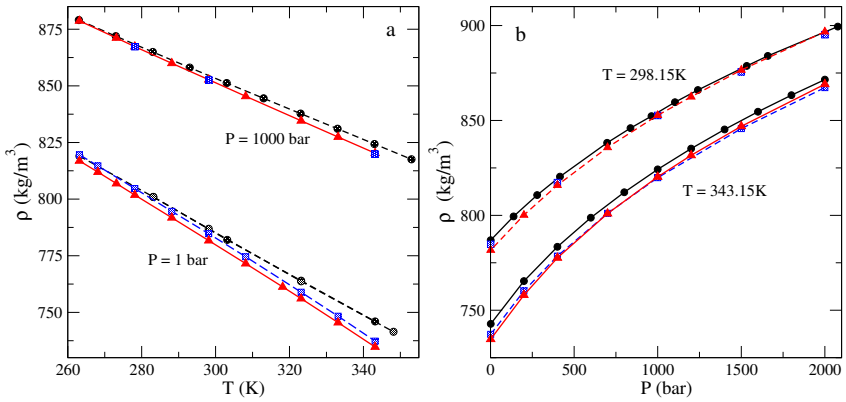

Figure 3. (Colour online) Panel a: Methanol density depending on temperature at pressure 1 bar, and at 1000 bar. The simulation results are for UAM-I united atom methanol model (red triangles) and TraPPE model (blue squares). The experimental data (black circles) at 1 bar are from Engineering toolbox and Kubota et al. [14], while at 1000 bar they are from [33]. Panel b: Methanol density depending on pressure at temperature 298.15 K and at 343.15 K. The experimental data are from [14] (298.15K) and [33] (343.15). Other notations as in panel a.

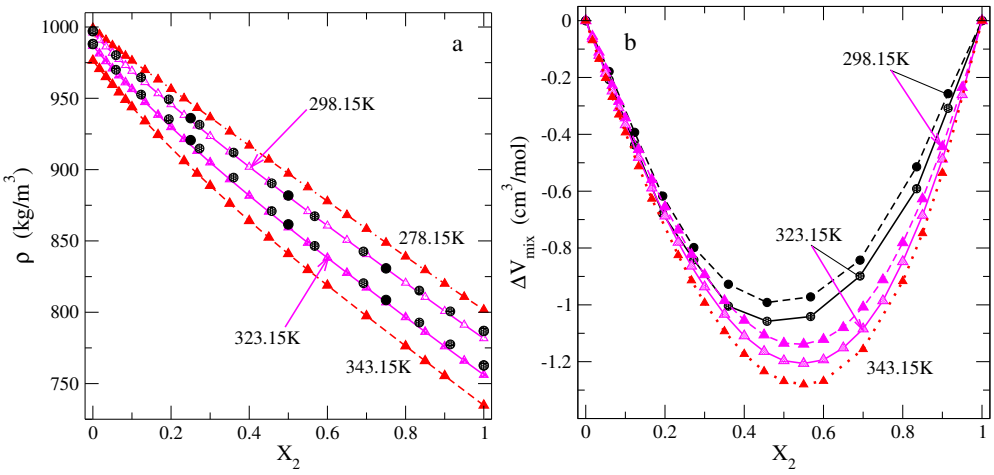

Figure 4. (Colour online) Panel a: Composition dependence of density of water-methanol mixtures at different temperatures, at a fixed pressure, $P = 1$ bar. The experimental data (black circles), at $T = 298.15$ K and 323.15 K, are from [14, 34], respectively. The simulation results (red and magenta triangles) are for TIP4P/ε — UAM-I model. Panel b: The excess mixing volume depending on composition at different temperatures at a fixed pressure, $P = 1$ bar. Experimental data are taken from [34].

We learn from figure 4a that the $\rho(X_2)$ dependencies at different temperatures behave similarly. They are almost linear curves descending from pure water to pure methanol values. From the limited comparison with experimental data, one can conclude that the behavior of density is reasonably correct. However, small inaccuracy of simulation models can be seen for methanol-rich mixtures.

It is important to correctly capture the deviation from ideality of a given property. This kind of insights follows, for example, from the excess mixing volume. The excess mixing volume is defined as follows, $\Delta V_{\text{mix}} = V_{\text{mix}} - X_2V_2 - (1 - X_2)V_1$, where V_{mix}, V_2 and V_1 refer to the molar volume of the mixture and of the individual components, methanol and water, respectively. Experimental data show that ΔV_{mix} is negative and exhibits a minimum at $X_2 \approx 0.45$, figure 4b. The simulation results show qualitatively similar trends of behavior. A comparison between the experiment and simulations with TIP4P/ε–UAM-I model shows that the model describes ΔV_{mix} for water-rich mixtures very well. At a higher alcohol content,

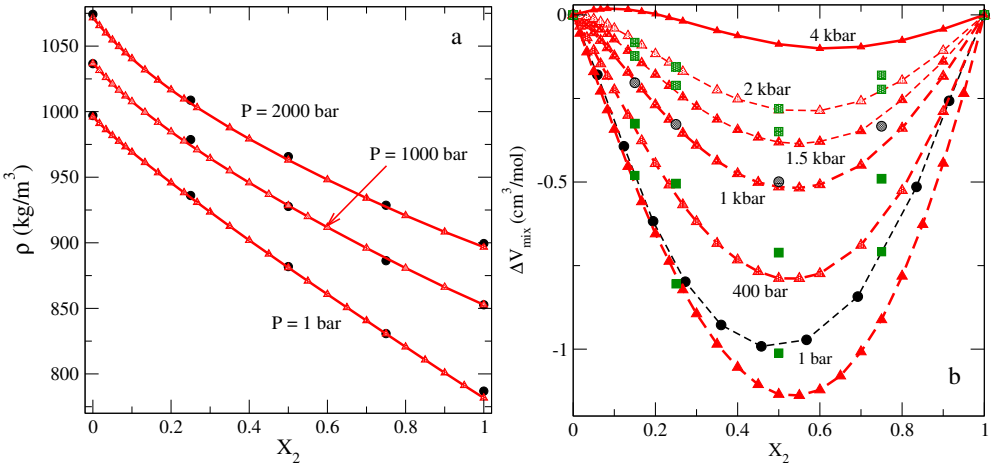

Figure 5. Panel a: Composition dependence of density of water-methanol mixtures at different pressures, P = 1 bar, 1000 bar, and 2000 bar at a fixed temperature 298.15 K (panel a). Panel b: Composition dependence of excess mixing volume at different pressures indicated in the figure at 298.15 K. Experimental data in panel b are from [34] (black circles) and from [15] (green squares).

$X_2 > 0.2$, the model overestimates the values for ΔV_{mix}. The minimum of the excess mixing volume from simulations is at $X_2 \approx 0.55$ at different temperatures under study. The values for the ΔV_{mix} at a fixed value for X_2 slightly increase in magnitude with increasing temperature, presumably due to the break of hydrogen bonds. The simulation model appropriately reproduces $\Delta V_{\text{mix}}(X_2)$ and its temperature changes. Thus, an overall performance of the model can be termed as satisfactory with qualitative accuracy. It would be fair to note that the TIP4P/2005–TraPPE model, studied by us previously, provides a better description of $\Delta V_{\text{mix}}(X_2)$ at a single studied temperature, T = 298.15 K and at P = 1 bar, cf. figure 2a of [3].

Now, we would like to perform similar analyses, as in figure 4, exploring the behavior of $\rho(X_2)$ at different pressures and at a fixed value of temperature, T = 298.15 K. The simulation results for the TIP4P/ε–UAM-I model are shown in figure 5a.

It follows that the density of the mixtures depending on composition at different pressures is described quite satisfactorily. Therefore, the excess mixing volume depending on composition at different pressures is satisfactory as well. Moreover, the agreement between computer simulation results and experimental data becomes better with increasing pressure. The location of the minimum of $\Delta V_{\text{mix}}(X_2)$ is also rather well captured by the model considered at high pressures. However, certain discrepancy is observed for methanol-rich mixtures.

In order to discern the contributions of each species into the excess molar volume and to obtain deeper insights into the geometric aspects of mixing depending on composition, both from experiments and simulations, one can resort to the notion of the apparent molar volume of the species rather than the excess molar volumes. The apparent molar volume for each species according to the definition is [42]: $V_\phi^{(1)} = V_1 + \Delta V_{\text{mix}}/(1 - X_2)$ and $V_\phi^{(2)} = V_2 + \Delta V_{\text{mix}}/X_2$. We elaborated the experimental density data from [34] and the results from our simulations to construct the plots shown in panels a, b, c and d of figure 6.

The TIP4P/ε–UAM-I model provides a quite accurate description of the composition behavior for $V_\phi^{(2)}$ in water-rich mixtures and in the entire composition range at a fixed pressure, P = 1 bar (figure 6a). The minimum of $V_\phi^{(2)}$ is predicted at a slightly lower methanol concentration, $X_2 \approx 0.1$ (T = 298.15 K), in comparison to the experimental result, $X_2 \approx 0.13$. The minimum becomes more pronounced if the temperature decreases from 298.15 K to 273.15 K. On the other hand, the minimum is hardly visible at 323.15 K and is absent at a higher temperature, 343.15 K. Moreover, the location of the minimum on composition axis shifts to lower values of X_2 upon increasing temperature. The level of accuracy of the

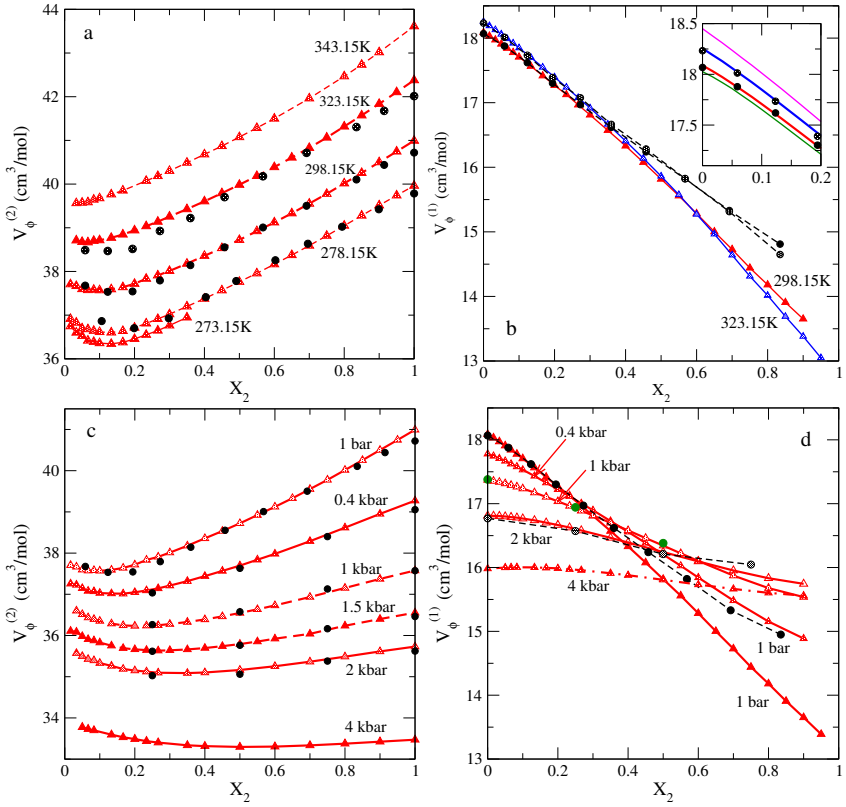

Figure 6. (Colour online) Panels a and b: A comparison of the composition dependence of the apparent molar volumes of methanol and water species from simulations, with the experimental data at different temperatures. The experimental data (black circles) are from [34] at 298.15 K and 323.15 K, and from Easteal et al. [35] at 278.15 K. The curves in the inset to panel b are for T = 278.15 K (green), T = 298.15 K (red), T = 323.15 K (blue) and T = 343.15 K (magenta). Panels c and d illustrate the behavior of the apparent molar volumes at different pressures. The temperature is fixed at 298.15 K.

present modelling is similar to the predictions of temperature trends for $V_\phi^{(2)}$ from TIP4P/2005–TraPPE model in figure 3a of [4].

Similar trends of behavior for $V_\phi^{(2)}$ are observed at different pressures, but at a fixed value of temperature, T = 298.15 K (figure 6c). The minimum of $V_\phi^{(2)}$ shifts to higher values of X_2 upon increasing pressure. The experimental data definitely confirm the existence of the minimum at 1 bar only. The lack of experimental data at higher pressures precludes to make conclusions even at a moderate pressure, P = 400 bar. We performed computer simulations up to P = 4 kbar to establish the existence of the limiting pressure at which the minimum ceases to exist. Still, the minimum of $V_\phi^{(2)}$ is observed at 4 kbar.

The behavior of $V_\phi^{(1)}$ depending on temperature and pressure in panels b and d of figure 6 is less illuminating. It is necessary to mention, however, that the simulation results agree well with the experimental data for mixtures with dominating water content only. By contrast, the model predictions deviate from the experimental results for $V_\phi^{(1)}$ in methanol-rich solutions. The change of inclination of $V_\phi^{(1)}$ on X_2 upon increasing temperature (figure 6b) or with increasing pressure (figure 6d), is well observed. However, interpretation of these trends would require a description of changes of the microscopic structure of water subsystem. Therefore, these observations will be revisited in the following publication on the subject.

In order to obtain a summarizing insight into the behavior of $V_\phi^{(2)}(X_2)$ in the entire pressure interval, we have reconsidered the simulation data from figure 6c and constructed a similar plot by using a

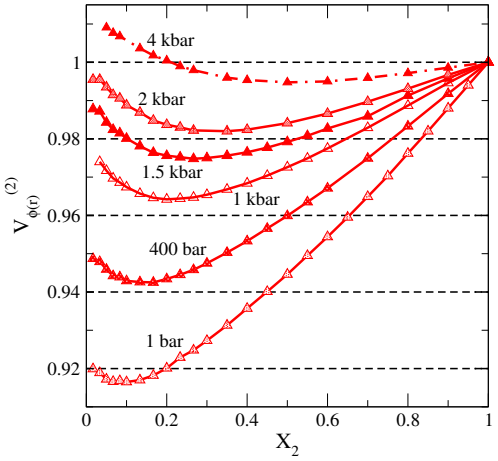

Figure 7. (Colour online) Composition dependence of the reduced apparent molar volume of methanol in water-methanol mixtures from simulations of TIP4P/ε–UAM-I model at different pressures. The temperature is fixed at 298.15 K.

reduced apparent volume of methanol species, $V^{(2)}_{\phi(r)}(X_2)$ (figure 7). It is defined as follows, $V^{(2)}_{\phi(r)}(X_2) = V^{(2)}_{\phi}(X_2)/V^{(2)}_{\phi}(X_2 = 1)$. From this kind of representation, one can see that at a high pressure, close to 4 kbar, the reduced apparent volume of alcohol species exhibits "crossover" from $V^{(2)}_{\phi(r)}(X_2) < 1$ behavior to $V^{(2)}_{\phi(r)}(X_2) > 1$, in the water-rich mixtures. In other words, expansion (with respect to the molar volume of pure methanol) rather than contraction is observed. It is difficult to interpret this behavior on its own, without referring to other properties.

In this aspect we would like to recall that the composition behavior of the apparent molar volume of alcohol species in water-rich mixtures can be related to the experimental results for abnormal intensity of scattered light [36–38]. Interestingly, it has been found that the Brillouin scattering behavior for water-methanol mixtures changes at $\approx$ 4 kbar according to the experiments discussed in [37]. These observations support the existence of a specific high pressure value leading to the peculiarities of geometric arrangement of species in water-methanol mixtures. Our simulation data confirm this fact in terms of $V^{(2)}_{\phi(r)}(X_2)$. In general terms, the simulation findings concerning the peculiarities of $V^{(2)}_{\phi}(X_2)$ behavior depending on T and P with a corresponding minimum, can urge the experimental work along this line of research.

3.3. Energetic aspects of mixing of ethanol and water molecules

Energetic manifestation of mixing trends is commonly discussed in terms of the excess mixing enthalpy, ΔH_{mix}. It is defined similar to the excess mixing volume above. We used the experimental results from [39–41] and our simulation data to explore ΔH_{mix} upon composition of water-methanol mixtures. The results are given in figure 8. It can be seen that ΔH_{mix} values coming from the simulation model are underestimated in comparison with experimental data at a low temperature, $T = 278.15$ K (panel a). However, this trend reverts at a higher temperature, $T = 323.15$ K. At this temperature, the model a bit overestimates the magnitude of values for ΔH_{mix} at compositions around minimum. Moreover, the minimum of ΔH_{mix} from simulation data is located at a higher X_2 compared to the experimental data. In summary, the model correctly predicts the temperature trends. The effect of attractive inter-molecular interactions decreases with increasing temperature. In other words, ΔH_{mix} values decrease in absolute values. The shape of $\Delta H_{\text{mix}}(X_2)$ is reproduced qualitatively correctly as well. However, the quantitative agreement of simulation results and experimental points is not reached at ambient pressure, $P = 1$ bar (panel a).

We were guided by the experimental data from [41] to perform simulations and construct a set of curves

in panel b of figure 8. These results illustrate the changes of balance between attractive and repulsive forces in the system upon the changes of temperature at a fixed pressure, $P = 400$ bar. According to the simulation predictions, the attractive forces still dominate at $T = 423.15$ K to yield negative values for $\Delta H_{\rm mix}$ in the entire composition interval. However, at a higher temperature, $T = 473.15$ K, $\Delta H_{\rm mix}$ is positive for all X_2. The experimental data indicate that such kind of change from exothermic to endothermic mixing occurs within the temperature interval between 373.15 K and 523.15 K. Unfortunately, intermediate experimental data are missing. On the other hand, it is difficult to establish the trends of behavior of the extremum, $\partial \Delta H_{\rm mix}/\partial X_2 = 0$ depending on temperature. The simulation predictions imply that the extremum composition increases with an increasing temperature in the temperature interval of negative values of $\Delta H_{\rm mix}$. Apparently, the "crossover" occurs in the methanol-rich mixtures. However, if the repulsive interactions become dominating in the system at $T = 473.15$ K, the extremum composition corresponds to $X_2 \approx 0.4$, i.e. for mixtures of the type $2MeOH - 3H_2O$. This kind of change, despite the experimental data being scarce, deserves a more extensive study using computer simulations at different values of pressure.

Concerning the trends of behavior of $\Delta H_{\rm mix}(X_2)$ at different pressures and at a fixed temperature, $T = 298.15$ K, one should note a reasonable agreement between simulations and experiment. It can be termed as satisfactory at a qualitative level. Namely, the dependence on pressure is correct within this pressure interval, the magnitude of $\Delta H_{\rm mix}(X_2)$ values increases upon increasing pressure from 1 bar to 400 bar. Indeed, the simulations predict this kind of behavior up to 2000 bar. However, in quantitative terms, the growth of magnitude of $\Delta H_{\rm mix}$ at minimum is modest. It mirrors the observations shown in the previous figure 6c for the minimum of the apparent molar volume of alcohol species. Probably, one should explore even higher values of pressure to intuitively capture a possible reversal of the $\Delta H_{\rm mix}$ behavior.

In order to elucidate the reasons of the discrepancy of modelling and experimental predictions for $\Delta H_{\rm mix}(X_2)$, it is worth to resort to the partial excess molar enthalpies. They follow from the excess mixing enthalpy, $\Delta H_{\rm mix}$ according to the definition [42],

$$h_{\rm ex}^{(1)} = \Delta H_{\rm mix} + X_2 \left(\frac{\partial \Delta H_{\rm mix}}{\partial X_1} \right) \Big|_{P,T}, \tag{3.1}$$

$$h_{\rm ex}^{(2)} = \Delta H_{\rm mix} - X_1 \left(\frac{\partial \Delta H_{\rm mix}}{\partial X_1} \right) \Big|_{P,T}, \tag{3.2}$$

where, $X_1 = 1 - X_2$.

In general terms, the computer simulation predictions for $h_{\rm ex}^{(2)}$ are reasonable at two values of temperature studied, $T = 278.15$ K and $T = 323.15$ K, as we see from figure 9a. On the other hand, the shape of $h_{\rm ex}^{(1)}$ from simulations agrees with experimental trends as well, figure 9a. The changes of inclination of $h_{\rm ex}^{(2)}$ on X_2 reflect the peculiarities of the energetics of mixing of methanol and water. At a low X_2, i.e., in the interval of water-rich mixtures, addition of even a small amount of alcohol species results in substantial changes of enthalpy (perhaps due to the changes of the hydrogen bonding network structure). On the other hand, at higher values of X_2, water species are much less bonded between themselves and provide a more comfortable medium for the incorporation of methanol molecules. Therefore, enthalpy changes are much less drastic. A "crossover" occurs at $X_2 \approx 0.3$, i.e., it starts at 1 MeOH - 2 H_2O composition. Concerning the absolute values of these partials, we observe a discrepancy between the simulations and experimental data. It is worth mentioning that in water-methanol mixtures, the magnitude of changes of $h_{\rm ex}^{(i)}$ on X_2 is much less drastic, in comparison to ethanol-water mixtures, i.e., for the alcohol with a larger hydrophobic tail, studied by us very recently [43]. In summary, the TIP4P/ε - UAM-I model provides a satisfactory description of the energetic trends of mixing of methanol and water species under such conditions.

Difficulties in the exploration of partial properties are illustrated in panel b of Figure 9. Namely, the partial derivatives of the excess mixing enthalpy are evaluated by using a restricted set of experimental points. As a result, noisy curves are obtained. On the other hand, one can use a more "chemical engineering procedure" by the development of desirably accurate, analytical polynomial expression for a given property and following a much easier differentiation. One example of this semi-empirical type of

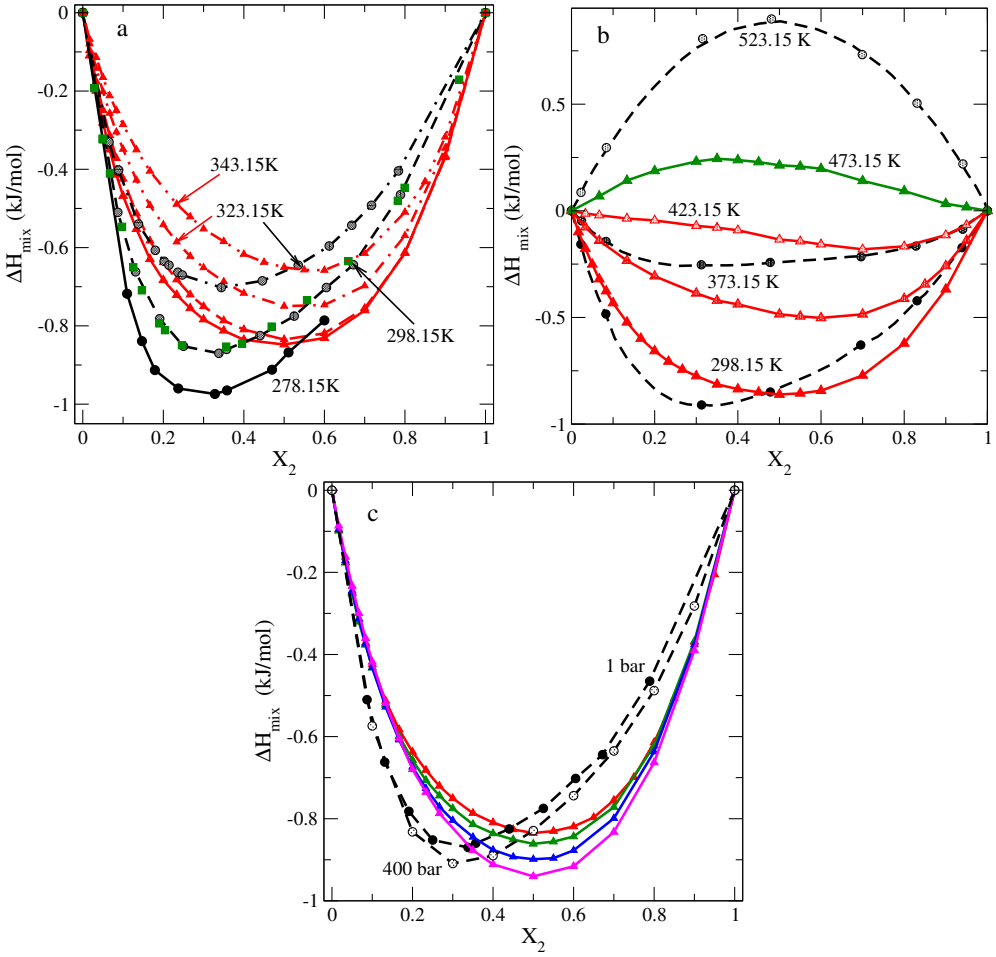

Figure 8. (Colour online) Panel a: A comparison of the behavior of the excess mixing enthalpy depending on temperature from simulations of TIP4P/ε–UAM-I model (red triangles) and experimental data (black circles at 323.15 K, 298.15 K, and 278.15 K) from [39]. Another set of experimental points (green squares) for 298.15 K are from [40]. The pressure is fixed at 1 bar. Panel b: Temperature changes of $\Delta H_{\rm mix}(X_2)$ from simulations, experimental data (black circles and polynomial fitting curves) were reproduced from figure 1c of [41] at 400 bar. Panel c: Pressure changes of $\Delta H_{\rm mix}(X_2)$ at a fixed temperature 298.15 K. The simulation data (triangles) are for the TIP4P/ε–UAM-I model at 1, 400, 1000 and 2000 bar from top to bottom (red, green, blue and magenta lines), respectively. The experimental data (circles) are from [39].

approach is the Tait equation of state for water density up to high pressures, see e.g., [44]. We hope to extend the present observations accumulating more data for enthalpy and to develop a more successful fitting procedure in a future work.

Our final remarks in this subsection concern the results shown in panel c of figure 9. The curves describe how the partial excess enthalpies of methanol and water species change with pressure at a fixed temperature, $T = 298.15$ K. The shape of each partial excess enthalpy does not change significantly upon increasing pressure from 1 bar to 1500 bar. Higher pressure leads to a more negative partials $h_{\rm ex}^{(1)}$ and $h_{\rm ex}^{(2)}$, in close similarity to our observation for the excess mixing enthalpy in figure 8c. Apparently, the value for composition, X_2, where change of slope of the partials occurs is not affected by pressure that seems to be quite high, $P = 1500$ bar. We are not able to prove whether this tendency remains at even higher pressures. Moreover, we have not found experimental data that confirm the predictions of simulations in this aspect. In summary, the energetic trends of mixing of alcohol species with water upon pressure changes require a more exhaustive laboratory and simulation investigations. At the moment, we

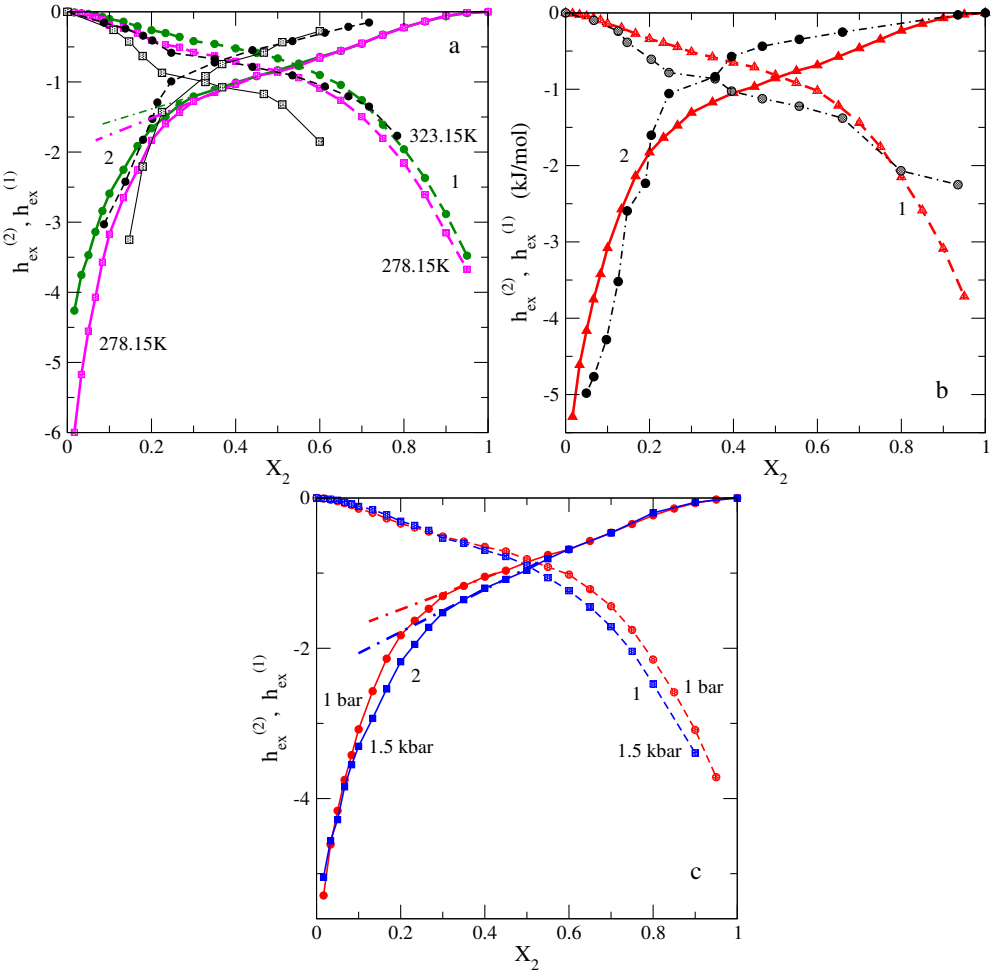

Figure 9. (Colour online) Panels a and b: A comparison of the behavior of the partial excess mixing enthalpies depending on temperature from simulations of TIP4P/ε–UAM-I model (green and magenta lines with symbols for 323.15 K and 278.15 K, respectively) and experiments (black lines with similar type of symbols). The experimental data are from [39] in panel a, and from [40] in panel b, respectively. In panel b — P = 1 bar, T = 298.15 K. Simulations — red triangles, experimental data — black circles. Panel c: The pressure dependence of partial excess molar enthalpies from simulations at 298.15 K.

note that the model predictions are in a qualitative agreement with the available experimental data.

3.4. Self-diffusion coefficients depending on temperature and pressure.

One of the most popular and stringent targets used in the design of the force fields and in testing properties for binary mixtures are the self-diffusion coefficients of species. They can be obtained from the mean square displacement of particles or from the calculations of the velocity auto-correlation functions. We calculate the self-diffusion coefficients, D_i ($i = 1, 2$), by the former route, via the Einstein relation,

$$D_i = \frac{1}{6} \lim_{t\to\infty} \frac{\mathrm{d}}{\mathrm{d}t} |\mathbf{r}_i(\tau + t) - \mathbf{r}_i(\tau)|^2, \tag{3.3}$$

where τ denotes the time origin. Default settings of GROMACS were used for the separation of the time origins.

Let us begin from the data for individual species. The experimental data for the self-diffusion coefficient of water depending on temperature have been taken from [45–47], panel a of figure 10. Both

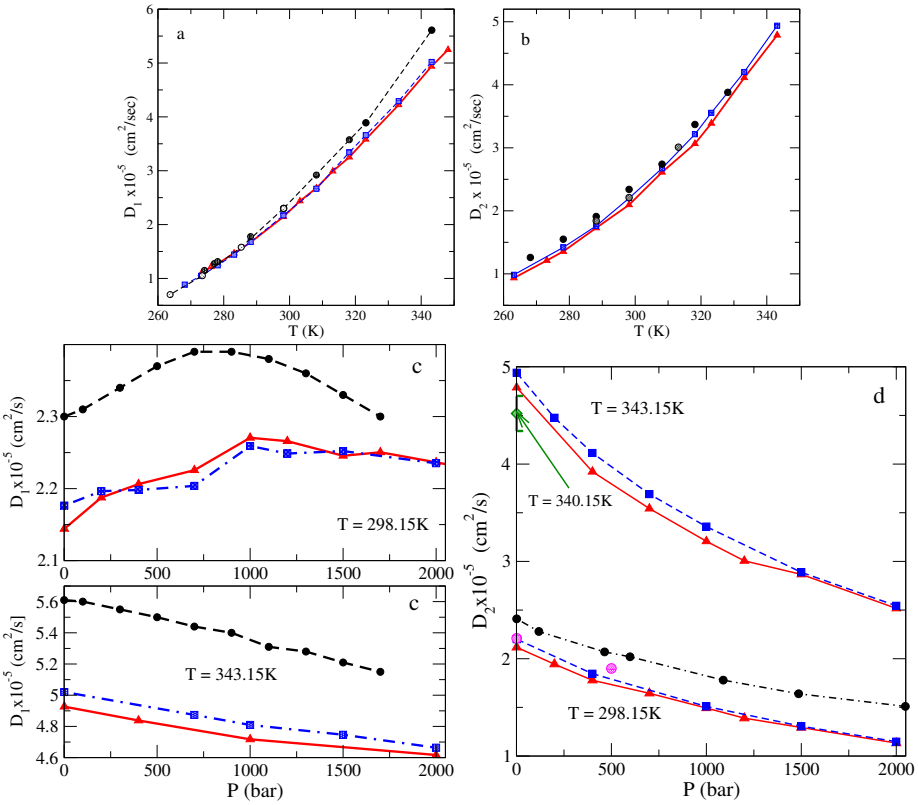

Figure 10. (Colour online) Panels a and b: Self-diffusion coefficients of water and methanol depending on temperature at ambient pressure. Red triangles and blue squares in panel a are for TIP4P/ε and TIP4P/2005 water models, respectively. The experimental data are from Krynicki et al. [45], Mills [46], and Gillen [47], respectively (circles with decreasing black colour intensity). In panel b: red triangles and blue squares are for UAM-I and TraPPE methanol models, respectively. The experimental data are from [48] and [49] (circles with decreasing black color intensity). Panel c: $D_1(P)$ from simulations of TIP4P/ε and TIP4P/2005 water models (the nomenclature of lines as in panel a). The experimental data are from [45] (black circles) Panel d: $D_2(P)$ from simulations of UAM-I and TraPPE methanol models at different temperatures. The experimental data are from [50] (black circles with dash-dotted line), from [49] (magenta circles), the green diamond with error bars is from [51]. The nomenclature of colours and lines for simulation results — as in panel a.

simulated models, TIP4P/2005 and TIP4P/ε, describe $D_1(T)$ quite well. Still, one observes that the $D_1(T)$ from simulations is underestimated in the temperature interval from $T \approx 300$ K up to 343.15 K, in comparison with experimental data. On the other hand, the UAM-I and TraPPE models for methanol describe $D_2(T)$ very well in the entire temperature range studied (figure 10b). The simulation data in both panels of figure 10 refer to $P = 1$ bar.

Now, let us inspect the dependencies $D_1(P)$ and $D_2(P)$ at a fixed temperature. For water we observe two types of behavior shown in figure 10c. At room temperature, 298.15 K, the self-diffusion coefficient, D_1, increases upon increasing pressure from 1 bar to $P \approx 700$ bar and then decreases with further growth of pressure. The simulation data, for both water models involved, exhibit similar trends. However, the maximum of $D_1(P)$ occurs at a higher value of pressure, $P \approx 1000$ bar, in comparison with the experimental results. The discrepancy between simulations and experiments is not big in absolute values in the entire interval of pressures. At a higher fixed temperature, 343.15 K, the simulations and experiments show that $D_1(P)$ smoothly decreases with increasing pressure. This kind of behavior is characteristic of simple liquids. Thus, in both water models, the effects of hydrogen bonding implicitly hidden in the self-diffusion coefficient are weak. On the other hand, at a lower room temperature, "a simple fluid"-like

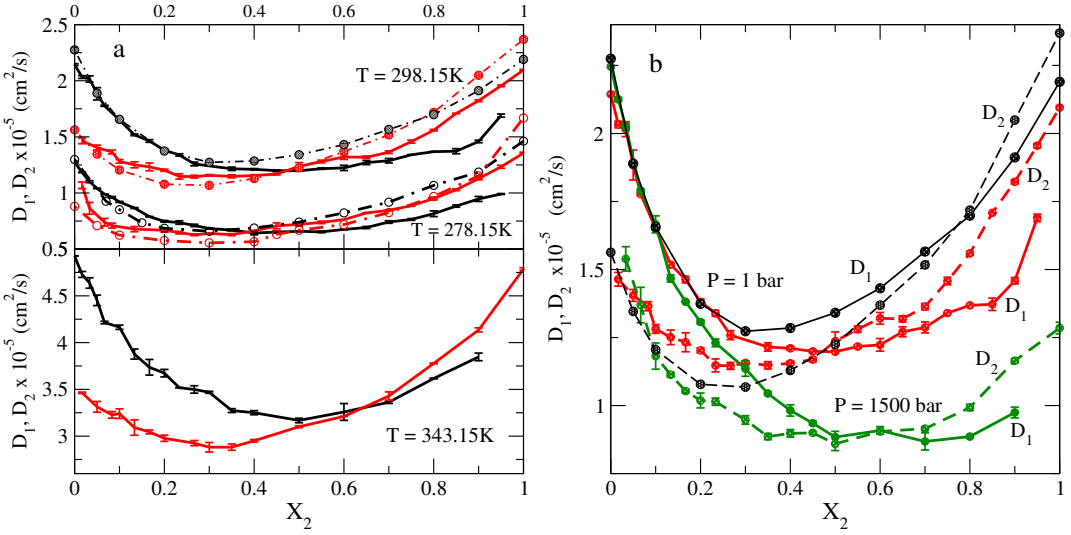

Figure 11. (Colour online) Panel a: Composition dependence of the self-diffusion coefficients of water and methanol at different temperatures at a fixed pressure $P = 1$ bar. The red and black curves correspond to methanol and water species, respectively. The experimental data in the upper part of panel a are marked by dash-dotted lines with circles [52]. Panel b: Composition dependence of the self-diffusion coefficients of water and methanol at different pressures at a fixed temperature 298.15 K. The solid and dashed lines correspond to water and methanol species, respectively. Black lines with circles — experimental data [52] at $P = 1$ bar. Red lines — 1 bar; green lines — 1500 bar.

behavior is observed solely at high pressures, probably because the hydrogen bonded network is severely damaged already at ≈ 700 bar.

In contrast to water, the self-diffusion coefficient of methanol, $D_2(P)$ monotonously decreases with increasing pressure at both fixed temperatures, 298.15 K and 343.15 K (figure 10d). Thus, the effects of bonding between methanol molecules are not strong under conditions of our study. Concerning the agreement between the predictions of two methanol models in question and experimental data, it can be termed as reasonable at 298.15 K. However, at a higher temperature of our interest, we have not found systematic data. Moreover, the point at $P = 1$ bar from [51] at 340.15 K is not definite. Other experimental techniques yield even a higher value for $D_2(P)$ at this pressure.

Now, we would like to turn our attention to water-mixture and explore the evolution of $D_i(X_2)$, $i = 1, 2$, with temperature and pressure. The simulation results and available experimental data are given in figure 11. From panel a of this figure, we learn that the composition dependence of the self-diffusion coefficients of both species from simulations is in qualitative agreement with the experimental data from [52] at 278.15 K and 298.15 K. The diffusion in water-rich mixtures is better described than in mixtures with higher concentration of alcohol species. Concerning the changes of magnitude of D_1 and D_2 with increasing temperature, we observe that the trends captured by simulated models are correct, as it follows from the inspection of available experimental data. However, the crossover composition value between the regions where $D_1 > D_2$ and where $D_1 < D_2$ is not accurately reproduced by the model under study. Similar observations are valid for the behavior of D_1 and D_2 upon increasing pressure. The trends of changes concerning the magnitudes of the self-diffusion coefficients are intuitively correct. However, we were unable to find laboratory data confirming the simulation predictions.

3.5. Summary and conclusions

To conclude, we report our fresh results concerning the trends of behavior of the mixing properties and self-diffusion coefficients of water-methanol liquid mixtures. They are studied dependent on the temperature, pressure and composition by using isobaric-isothermal molecular dynamics simulations.

This study is just the first part of the ampler project that implies an investigation of the microscopic structure in terms of various pair distribution functions, coordination numbers and hydrogen bonding network evolution. Besides, we contemplate to explore the dynamic behavior of the mixtures in question in terms of viscosity and various relaxation times, dielectric and interfacial properties. Progress of research along these lines will be reported in separate publications. The mixtures in question are considered by using the recently proposed parametrization within the TIP4Pε–UAM-I model. In the case of pure components, we have involved the TIP4P/2005 water model as well as the TraPPE methanol model. However, in the case of mixtures, solely a single combination of water and methanol modelling has been considered for the moment. Evaluation of the performance of different combinations of models is postponed to future work. The motivation of using the present version of the model for mixtures has two reasons. On the one hand, a possible extension to other monohydric alcohols aqueous solutions depending on temperature and pressure is ensured, as we showed in part in our recent work [26]. On the other hand, in order to put closer the simulation outputs and several laboratory works by using dielectric spectroscopy, one would need a confiable description of the dielectric constant, at least. Temperature dependence of the dielectric constant of water is satisfactory within the TIP4Pε modelling as shown in [23]. Thus, the present modelling is quite promising for water-alcohol mixtures.

Most interesting and presumably important findings of the present work are as following. Concerning the temperature trends of the apparent molar volume of methanol species, we have shown that the minimum of $V_{\phi}^{(2)}$ disappears with increasing temperature in the interval between 323.15 K and 343.15 K. Moreover, the dependence of the most favourable contraction of the volume on temperature is reproduced by simulations as well. Pressure trends of this property exhibit an interesting evolution as well. Namely, the minimum of $V_{\phi}^{(2)}$ is observed at all pressures, upon increasing it up to 4 kbar. However, at a high pressure close to 4 kbar, we observe a crossover for the mixing volume, ΔV_{mix}, from negative to positive values. This implies an expansion of the volume in water-rich mixtures, in contrast to the contraction observed in mixtures with a higher amount of alcohol (methanol). Consequently, the reduced apparent molar volume of methanol species becomes a bit larger than 1 at low X_2 values. This trend of behavior is definitely related to the evolution of the hydrogen bonds network upon adding alcohol to water. A set of issues related to this finding, or say its interpretation, will be discussed elsewhere in the studies of microscopic structure. One more interesting trend, resulting from our calculations, is the change of the excess mixing enthalpy upon increasing temperature. Namely, the computer simulation results of the model evidence the changes from the exothermic to endothermic mixing in the temperature interval from 423.15 K to 473.15 K. In qualitative terms, this finding is in agreement with the experimental data.

Finally, we have performed a rather detailed investigation of the behavior of self-diffusion coefficients depending on temperature and pressure for individual species and for the mixtures in the entire range of composition. We observed that the dependence of the self-diffusion coefficient of water on pressure is different at room temperature, 298.15 K, and at a higher temperature, 343.15 K. Namely, the $D_1(P)$ (1 refers to water) increases if pressure grows from 1 bar to $\approx$ 1 kbar and then decreases with the further increasing pressure, at $P > 1$ kbar, if $T = 298.15$ K. At a high temperature, $T = 343.15$ K, $D_1(P)$ monotonously decreases upon increasing pressure. These changes of the behavior for $D_1(P)$ are related to the evolution of hydrogen bonding structure of water. On the other hand, the self-diffusion coefficient of methanol decreases with increasing pressure in the entire interval of temperature and pressure studied, as expected. These trends are then manifested in the evolution of $D_1(X_2)$ and $D_2(X_2)$ at different thermodynamic states, determined by T and P. The accuracy of these predictions is difficult to evaluate at the moment because the experimental data are scarce.

Acknowledegments

The authors acknowledge support by CONAHCyT of Mexico under the grant CBF2023-2024-2725. Helpful discussions with Dr. Laszlo Pusztai stimulated this work. Technical support of Magdalena Aguilar at Institute of Chemistry of the UNAM is acknowleged as well. We express our gratitude to all of them.

References

1. Galicia-Andrés E., Pusztai L., Temleitner L., Pizio O., J. Mol. Liq., 2015, **209**, 586, doi:10.1016/j.molliq.2015.06.045.
2. Galicia-Andres E., Dominguez H., Pusztai L., Pizio O., J. Mol. Liq., 2015, **212**, 70, doi:10.1016/j.molliq.2015.08.061.
3. Cruz Sanchez M., Dominguez H., Pizio O., Condens. Matter Phys., 2019, **22**, 13602, doi:10.5488/CMP.22.13602.
4. Cruz Sanchez M., Aguilar M., Pizio O., Condens. Matter Phys., 2020, **23**, 34601, doi:10.5488/CMP.23.34601.
5. Sun Q., Molecules, 2022, **27**, 7009, doi:10.3390/molecules27207009.
6. Grigera J. R., McCarthy A. N., Biophys. J., 2010, **98**, 1626, doi:10.1016/j.bpj.2009.12.4298.
7. Ghosh T., García A. E., Garde S., J. Am. Chem. Soc., 2001, **123**, 44, 10997, doi:10.1021/ja010446v.
8. Hummer G., Garde S., Garcia A. E., Pratt L. R., Proc. Natl. Acad. Sci. U. S. A., 1998, **95**, 1552, doi:10.1073/pnas.95.4.1552.
9. Oakenfull D., Fenwick D. E., J. Chem. Soc., Faraday Trans. 1, 1979, **75**, 636, doi:10.1039/F19797500636.
10. Temleitner L., Hattori T., Abe J., Nakajima Y., Pusztai L., Molecules, 2021, **26**, 1218, doi:10.3390/molecules26051218.
11. Yamaguchi T., Benmore C. J., Soper A. K., J. Chem. Phys., 2000, **112**, 8976, doi:10.1063/1.481530.
12. Yoshida K., Ishida S., Yamaguchi T., Mol. Phys., 2019, **117**, 3297, doi:10.1080/00268976.2019.1633481.
13. Sato T., Chiba A., Nozaki R., J. Chem. Phys., 2000, **113**, 9748, doi:10.1063/1.1321767.
14. Kubota H., Tsuda S., Murata M., Yamamoto T., Tanaka Y., Makita T., Rev. Phys. Chem. Jpn., 1980, **49**, 59.
15. Kubota H., Tanaka Y., Makita T., Int. J. Thermophys., 1987, **8**, 47, doi:10.1007/BF00503224.
16. Moghaddam M. S., Chan H. S., J. Chem. Phys., 2007, **126**, 114507, doi:10.1063/1.2539179.
17. Koga K., J. Chem. Phys., 2004, **121**, 7304, doi:10.1063/1.1792571.
18. Chau P.-L., Mancera R. L., Mol. Phys., 1999, **96**, 109, doi:10.1080/00268979909482943.
19. Hernández-Cobos J., Ortega-Blake I., J. Chem. Phys., 1995, **103**, 9261, doi:10.1063/1.469986.
20. Durell S. W., Ben-Naim A., J. Phys. Chem. B, 2021, **125**, 13137, doi:10.1021/acs.jpcb.1c07802.
21. Abascal J. L. F., Vega C., J. Chem. Phys., 2005, **123**, 234505, doi:10.1063/1.2121687.
22. Gonzalez-Salgado D., Vega C., J. Chem. Phys., 2016, **145**, 034508, doi:10.1063/1.4958320.
23. Fuentes-Azcatl R., Alejandre J., J. Phys. Chem. B, 2014, **118**, 1263, doi:10.1021/jp410865y.
24. Chen B., Potoff J. J., Siepmann J. I., J. Phys. Chem. B, 2001, **105**, 3093, doi:10.1021/jp003882x.
25. García-Melgarejo V., Núñez-Rojas E., Alejandre J., J. Mol. Liq., 2021, **323**, 114576, doi:10.1016/j.molliq.2020.114576.
26. Méndez-Bermúdez J. G., Pizio O., J. Mol. Liq., 2025, **421**, 126789, doi:10.1016/j.molliq.2024.126789.
27. Spoel D., Lindahl E., Hess B., Groenhof B., Mark A. E., Berendsen H. J. C., J. Comput. Chem., 2005, **118**, 1701, doi:10.1002/jcc.20291.
28. Holten V., Sengers J. V., Anisimov M. A., J. Phys. Chem. Ref. Data, 2014, **43**, 043101, doi:10.1063/1.4895593.
29. Dzhavadov L. N., Brazhkin V. V., Fomin Yu. D., Ryzhov V. N., Tsiok E. N., J. Chem. Phys., 2020, **152**, 154501, doi:10.1063/5.0002720.
30. Pi H., Aragones J. L., Vega C., Noya E. G., Abascal J. L. F., Gonzalez M. A., McBride C., Mol. Phys., 2009, **107**, 365, doi:10.1080/00268970902784926.
31. Hare D. E., Sorensen C. M., J. Chem. Phys., 1987, **82**, 4840, doi:10.1063/1.453710.
32. Fine R. A., Millero F. J., J. Chem. Phys., 1973, **59**, 5529, doi:10.1063/1.1679903.
33. Linstrom P. J., Mallard W. G. (Eds.), NIST Chemistry WebBook, NIST Standard Reference Database 69, National Institute of Standards and Technology, Gaithersburg MD, 2025, doi:10.18434/T4D303.
34. Mikhail S. Z., Kimel W. R., J. Chem. Eng. Data, 1961, **6**, 533, doi:10.1021/je60011a015.
35. Easteal A. J., Woolf L. A., J. Chem. Thermodyn., 1985, **17**, 49, doi:10.1016/0021-9614(85)90031-X.
36. Sato M., Ike Y., Kano J., Kojima S., AIP Conf. Proc., 2006, 832 , 291, doi:10.1063/1.2204509.
37. Jiménez-Ruiz M., Jiménez-Riobóo R. J., Tissen V., Ramos M. A., Schober H.,Phys. Status Solidi C, 2004, **1**, 3178, doi:10.1002/pssc.200405281.
38. Blaudez D., Mallamace F., Micali N., Trusso S., Vasi C., Il Nuovo Cimento D, 1994, **16**, 923, doi:10.1007/BF02456743.
39. Tomaszkiewicz I., Randzio S. L., Gierycz P., Thermochim. Acta, 1986, **103**, 281, doi:10.1016/0040-6031(86)85164-4.
40. Lama R. F., Lu B. C.-Y., J. Chem. Eng. Data, 1965, **10**, 216, doi:10.1021/je60026a003.
41. Simonson J. M., Bradley D. J., Busey R. H., J. Chem. Thermodyn., 1987, **19**, 479, doi:10.1016/0021-9614(87)90145-5.
42. Tôrres R. B., Marchiore A., Volpe P., J. Chem. Thermodyn., 2006, **38**, 526, doi:10.1016/j.jct.2005.07.012.
43. Benavides Bautista D., Aguilar M., Pizio O., Condens. Matter Phys., 2024, **27**, 23201,

doi:10.5488/CMP.27.23201.
44. Dymond J. H., Malhotra R., Int. J. Thermophys., 1988, **9**, 941, doi:10.1007/BF01133262.
45. Krynicki K., Green C. D., Sawyer D. W., Faraday Discuss. Chem. Soc., 1978, **66**, 199, doi:10.1039/DC9786600199.
46. Mills R., J. Phys. Chem., 1973, **77**, 685, doi:10.1021/j100624a025.
47. Gillen K. T., Douglass D. C., Hoch M. J. R., J. Chem. Phys., 1972, **57**, 5117, doi:10.1063/1.1678198.
48. Rathbun R. E., Babb A. L., J. Phys. Chem., 1961, **65**, 1072, doi:10.1021/j100824a520.
49. Hiraoka H., Izui Y., Odugi J., Jono W., Rev. Phys. Chem. Japan, 1958, **28**, 61.
50. Hurle R. L., Easteal A. J., Woolf L. A., J. Chem. Soc. Faraday Trans. I, 1985, **81**, 769, doi:10.1039/F19858100769.
51. Asahi N., Nakamura Y., J. Chem. Phys., 1998, **109**, 9879, doi:10.1063/1.477656.
52. Derlacki Z. J., Easteal A. J., Edge A. V. J., Woolf L. A., Roksandic Z., J. Phys. Chem., 1985, **89**, 5318, doi:10.1021/j100270a039.

Про вплив температури, тиску і складу водно-метанольних сумішей на їх властивості. I. Густина, надлишковий об'єм змішування та ентальпія, а також коефіцієнти самодифузії, отримані методом молекулярної динаміки.

М. Круз Санчес[1], В. Трехос Монтоя[1], О. Пізіо[2]

[1] Хімічний факультет Автономного університету Метрополітана-Істапалапа, просп. Сан Рафаель Атлікско 186, 09340, CDMX, Мехіко

[2] Інститут Хімії, Національний Автономний Університет Мексики, Мехіко

З використанням комп'ютерного моделювання в рамках ізобарно-ізотермічної молекулярної динаміки, досліджено залежність деяких основних властивостей модельних сумішей води та метанолу від температури, тиску та хімічного складу. Основна увага зосереджена на неполяризаційній моделі UAM-I-EW об'єднаного атома метанолу, яка нещодавно була параметризована у V. Garcia-Melgarejo та ін. [J. Mol. Liq., 2021, **323**, 114576], у поєднанні з моделлю води TIP4P/ε. У перспективі, модель метанолу дозволяє зручне узагальнення теорії на випадок інших одноатомних спиртів, змішаних з водою. Описано поведінку густини, надлишкового об'єму змішування та ентальпії; інтерпретуються властивості часткового змішування. Крім того, досліджено тенденції поведінки коефіцієнтів самодифузії частинок суміші. Якість модельних передбачень критично оцінюється шляхом детального порівняння з експериментальними результатами. Отримані результати є новими та дають змогу зрозуміти поведінку подібних сумішей при різних температурах та високих тисках. Обговорюється вдосконалення моделювання, необхідне для подальших досліджень.

Ключові слова: *моделювання методом молекулярної динаміки, суміші води та метанолу, парціальний молярний об'єм, надлишкова ентальпія, коефіцієнти самодифузії*